A quantitative study of carbon monoxide and carbon dioxide evolution during thermal degradation of flame retarded epoxy resins

Bhaskar Biswas, Baljinder K Kandola*, A Richard Horrocks, Dennis Price

Centre for Materials Research and Innovation, University of Bolton, Deane Road, Bolton, BL3 5AB, UK.

Abstract

Thermogravimetry (TGA) combined with infrared analysis of the evolved gases (EGA) has been used to study the thermal degradation behaviour of epoxy resin both in air and nitrogen. The mass loss as a function of temperature has been correlated with the evolution of carbon monoxide (CO) and carbon dioxide (CO_2), and oxygen consumption as measured using an oxygen analyser. An analytical technique has been developed to quantitatively measure the carbon monoxide and dioxide gases evolved. The effect of a range of flame retardants containing phosphorus, nitrogen and halogen elements on CO and CO_2 evolution during thermal degradation of flame retarded epoxy resins has also been observed.

Keywords : Epoxy resin; Flame retardants; TGA; EGA; Carbon dioxide; Carbon monoxide

* Corresponding author. Tel. : +44 1204 903517 ; fax : +44 1204 399074
E-mail address : b.kandola@bolton.ac.uk (B.K.Kandola)

1. Introduction

Organic polymers when exposed to heat, decompose and their decomposition products burn generating various fire gases and smoke. Invariably the products of combustion are highly toxic and the cause of most fire fatalities [1]. The prime toxic product is carbon monoxide (CO) accompanied with asphyxiont, carbon dioxide (CO_2). Fire gas toxicity is dependent upon material composition and the fire conditions [2]. The formation of CO in fires occurs at low temperatures in the early stages of fire development mainly due to incomplete combustion of the pyrolysed polymer volatile fuels. As the fire develops, the higher temperature favours the formation of CO_2, which is particularly dependent on oxygen availability to the fire [3]. The evaluation of the polymer flammability is carried out using a variety of techniques, most of which do not correlate well with each other. They tend to fall into two classes, namely those which are product-based (e.g. the UL 94 (ISO 1210) [4] for assessing bulk polymer behaviour) and science based (e.g. the Limiting Oxygen Index (ISO 4589) [5] and Cone Calorimeter tests (ISO 5660)) [6]. Such test methods usually measure parameters such as ease-of-ignition, ease-of-extinction, rate of burning, the effect of oxygen concentration and heat release rate. All these techniques involve different sample sizes and need a few replicate tests for reliable results and none yield fundamental information regarding the mechanism of thermal degradation that underpins the burning process. Thermal analytical techniques, which involve only few milligrams of sample, are quite often used during new polymer developmental stages, because they give information about physical and chemical changes occurring on heating the polymer in a controlled atmosphere. Although thermal analytical results do not correlate with actual fire conditions, they give insight into mechanisms of thermal

degradation, in particular when evolved gases are characterised analytically [7-14]. In this work a thermogravimetric analyser coupled with infrared analysers has been used to quantitatively measure the CO and CO_2 produced during thermal degradation of a typical epoxy resin of aerospace grade.

Thermoset epoxy resins are widely used in a variety of areas like aerospace, marine, automobile, adhesive and coating industries [15, 16]. Chemically, epoxy resins may have variety of structures [15-17] but all contain epoxide groups () in their polymeric backbone. Like other organic polymers, epoxy resins can be flame retarded either by incorporating flame retardant additives or by copolymerization with reactive flame retardants [18]. In this work selected flame retardants (e.g. phosphorous – nitrogen, organophosphorous and halogen based) have been added to the resin prior to polymerization. The TGA-EGA technique has been used to give a chemical insight into the thermal decomposition of the different flame retardant resins.

2. Experimental

2.1 Materials

Chemicals used for calibration of EGA instrumentation :

(i) Sodium bicarbonate, $NaHCO_3$ (Supercook, UK)

(ii) Calcium carbonate, $CaCO_3$ - (Sigma Chemical Co., USA)

Resin :

Epoxy resin : Triglycidyl-p-aminophenol (Vantico Ltd., UK)

Curing agent : 4,4 Diamino diphenyl sulphone, DDS (Acros Organics BVBA, Belgium)

Thermoplastic toughener: Polyether sulphone, PES (Cytec, Netherlands)

Flame retardants : These were selected based on the following criteria – they should contain phosphorous and/or nitrogen; if bromine is present, P or N should be also and they should be compatible with the resin. The following were selected as a consequence :

Phosphorous and nitrogen based :

(i) Ammonium polyphosphate, APP (Antiblaze MC, Rhodia Specialities Ltd., UK)

(ii) Melamine phosphate, MP (Antiblaze NH, Rhodia Specialities Ltd., UK)

(iii) Melamine pyrophosphate, MPP (Antiblaze NJ, Rhodia Specialities Ltd., UK)

Organophosphorous based :

(iv) Resorcinol bis-(diphenyl phosphate), RDP (Chemtura, UK)

(v) Bisphenol A bis-(diphenyl phosphate), BAPP (Chemtura, UK)

Halogen based :

(vi) Tris(tribromoneopentyl)phosphate, FR 372 (DSBG, Israel)

(vii) Tris(tribromophenyl)cyanurate, FR 245 (DSBG, Israel)

2.2. Sample Preparation

Epoxy resin samples with and without flame retardants have been formulated by a hot-melt method. The epoxy resin was heated to 120^{o}C to melt it and toughener and required amounts of flame retardants were added slowly while stirring with a mechanical stirrer. The mixture was further stirred for 30 minutes. The temperature was lowered to 100^{o}C, the curing agent DDS added and the mixture stirred at 100^{o}C for 30 minutes in order to

yield a homogeneous mixture. The mixture was then degassed at 85^{o}C for two hours. Small quantities (~ 200 mg) of uncured samples were stored for thermal analytical tests and the rest poured in aluminium moulds to cure for further flammability testing (results to be published in a forthcoming publication) [19]. The sample compositions are given in Table 1 and different samples prepared are listed in Table 2.

2.3. Equipment

The TGA experiments were carried out using a Polymer Laboratories TG 1000 instrument under flowing air or nitrogen atmosphere at 20 ml/min gas flow rate and heating rate of 10^{o}C/min from room temperature to 900^{o}C. About 2 -3 mg sample was used. The TGA instrument was connected in series to gas analysers (O_2, CO and CO_2) manufactured by Irridium, City technology, UK, via an unheated gas line. CO and CO_2 were monitored using a non dispersive infrared analyser operating at 2000-2300 cm^{-1} wavelength and oxygen with an electrochemical sensor.

3. Results and Discussion

3.1 Calibration of the TGA-EGA equipment

The combined TGA-EGA experiment has been calibrated using gases quantitatively derived from chemicals with known thermal degradation mechanisms, namely sodium bicarbonate ($NaHCO_3$) and calcium carbonate ($CaCO_3$).

During TGA-EGA experiments, the TGA records changing mass of a sample with respect to time or temperature, while the gas analyser records evolved gas concentrations as percentage volume concentrations (e.g. CO, CO_2, O_2) in the purge gas with respect to

time. The relationship between time and temperature can be drawn from the heating rate in TGA. In this work, the heating rate has been kept at 10^oC per minute and so

10^oC increment in TGA = 1 minute or 60 s period in the gas analyser

The time delay or transfer time [20] between the generation of gases in TGA and the detection of gases in gas analyzer has been measured by injecting CO_2 into the TGA and measuring the span of time until it is detected in the gas analyser [21] as shown in Fig. 1. A time delay of 28 s was observed at the purge gas flow rate of 20 ml/min.

The compiled TGA-EGA curves after compensating for 28s time delay for 5-7 mg $NaHCO_3$ and $CaCO_3$ decomposition are shown in Figs. 2 (a) and (b), respectively.

Sodium bicarbonate ($NaHCO_3$) decomposes at 110^oC producing CO_2 and water :

$$2NaHCO_3 \longrightarrow Na_2CO_3 + CO_2 + H_2O$$

and calcium carbonate ($CaCO_3$) decomposes around 700^oC producing CO_2 :

$$CaCO_3 \longrightarrow CaO + CO_2$$

As seen from above reactions, during decomposition of $NaHCO_3$ and $CaCO_3$, there is no consumption of oxygen. However, from Figs. 2(a) and (b), slight depletion in oxygen gas concentrations are observed. This can be seen more clearly in Fig. 3 where the graph for $NaHCO_3$ is replotted on a magnified scale. This depletion is most likely be due to dilution

of oxygen in the purge gas by the evolved CO and CO_2 as discussed below and needs to be considered if accurate measurement of oxygen consumption is to be achieved during degradation of polymer samples.

Oxygen dilution :

When a chemical degrades thermally, it produces some gaseous species, which add to the purge gas. Therefore this varies the total volume of purge gas, which alters the level of oxygen concentration. The oxygen concentration can be measured as shown below using the defined parameters,

Volume of total purge gas flow per second = f

Volume of oxygen in purge gas per second = f_{O_2}

Volume of CO_2 generation per second = f_{CO_2}

Volume of CO generation per second = f_{CO}

Calculated volume of gas flow per second, $F_{Cal} = f + f_{CO_2} + f_{CO}$

Initially at time = 0 s, there is no reaction and no carbon monoxide or carbon dioxide has been generated to give:-

$$f_{CO_2} = 0, \quad \text{and} \quad f_{CO} = 0$$

Hence, $F_{Cal} = f$

Concentration of oxygen = $\frac{f_{O_2}}{F_{Cal}} \times f = \frac{f_{O_2}}{f} \times f \approx 20.94\%$

During any stage of reaction at time = t_s ,

$$F_{Cal} = f + f_{CO_2} + f_{CO}$$

As CO and CO_2 are produced, these gases mix with the purge gas, thus raising the instantaneous total volume of gas flow through transfer line.

Hence, as F_{cal} increases at any instant, so f_{o_2} decreases.

Therefore, at any given time, the concentration of oxygen = $\frac{f_{O_2}}{F_{Cal}} \times f$

$$= \frac{f_{O_2}}{f + f_{CO_2} + f_{CO}} \times f < 20.94\%$$

With the help of above equation, percentage of oxygen concentration level has been calculated at each time for $NaHCO_3$ and $CaCO_3$ as shown by dotted lines in Figs. 2(a) and (b), and for clarity in Fig. 3 The calculated curve overlaps the experimental curve (solid line).

Oxygen consumption measurement :

From above discussion it is clear that the experimental curves for oxygen concentration include the dilution of oxygen by evolved gases. Therefore, by superimposing the experimental curve and calculated oxygen depletion curve, the equation of actual oxygen consumption can be derived from the difference between these curves, when a polymer sample is being oxidised during a TGA-EGA experiment.

The total O_2 consumption = $\sum_{i=p}^{q} (Dep\ O_2)_i - \sum_{i=p}^{q} (Obs\ O_2)_i$

Where, $Dep\ O_2$ = the calculated depletion level of oxygen per second

$Obs\ O_2$ = observed O_2 level per second, which is lower than $Dep\ O_2$

i = each point of baseline of the curve,

p = Starting point of the curve and

q = ending point of the curve.

CO-CO_2 measurement :

The CO-CO_2 gas analysers have been calibrated by verifying the concentration of flowing gas of known history from a gas cylinder. The CO-CO_2 analyser was precalibrated before every measurement. The production of CO, CO_2 gases has been calculated from the area under the curve by trapezoidal method or integration. Fig. 4 shows a typical curve for gas (CO or CO_2) generated in the EGA experiment.

From the curve, the CO_2 generation per second, at any time t is :

$$G_{CO_2} = \frac{f_{CO_2}}{F_{Cal}} \times F_r$$

Where, F_r is the experimental flow rate in ml/min (purge gas flow rate measured for evolved gas with a flow meter), which is compensated by maintaining a constant flow rate.

Therefore, the total CO_2 generation = $\sum_{i=p}^{q} (G_{CO_2})_i$,

Where, i = each point of baseline of the curve,

p = Starting point of the curve and

q = ending point of the curve.

This equation can also be applied for CO generated from the TGA.

The above methods have been used to calculate CO and CO_2 generated from sodium bicarbonate ($NaHCO_3$) and calcium carbonate ($CaCO_3$) in air and nitrogen and the results are given in Table 3. $NaHCO_3$ produces 26% by mass CO_2 and $CaCO_3$ by mass 44%, which are as expected. These values are unaffected by changing the medium from air to nitrogen as expected from their degradation mechanisms. This approach has been used to quantify gas evolution measurements from epoxy resin samples modified with different flame retardants.

3.2 Oxygen consumption and CO and CO_2 measurement for epoxy resin

TGA-EGA curves for the epoxy resin in air and nitrogen are shown in Fig. 5 and TGA and EGA analyses are given in Tables 4 and 5, respectively. For calculation of CO and CO_2 evolution, the thermal degradation mechanism discussed in details elsewhere [22], has been simplified as follows :

$$\text{Epoxy with / without FR} + O_2 \xrightarrow[\text{Air}]{\text{Heat}} CO_2 + CO + \text{Other volatiles} + \text{Char}$$

The above equation denotes a mass transport of materials in conjunction with oxygen diffusion into gaseous species and carbonaceous char. From the above equation, the sum of masses of reactants is considered as total input for the reaction. The mass of each product is measured w.r.t. total input of reactants. The CO and CO_2 values in Table 5 have been calculated, expressed as percentage, whereas the oxygen consumption is measured w.r.t. mass of the specimen (epoxy without/with FRs) and expressed as a percentage. All the results are given in Table 5. There is also a relationship between the

input and products. The percentages of CO and CO_2 are inversely proportional to total oxygen consumed while the weight of the specimens have been kept more or less constant. The production of CO and CO_2 commences during the second stage in air. This is discussed in following sections.

3.3 Thermal degradation behaviour of epoxy resin and analysis of evolved gases

TGA-EGA curves for the pure epoxy uncured resin are shown in Fig. 5, where it can be seen that in air it degrades in three stages; (i) first stage due to water loss through curing and dehydration (upto ~265 ^{o}C) with 10% mass loss, (ii) decomposition to a char (~350 - 460 ^{o}C) with 30% mass loss and (iii) char oxidation stage (~ 440 - 620 ^{o}C) [22,23] with 57% mass loss leaving 2.5 % char residue at the end. The exact temperature ranges for these three stages of the resin as obtained from TGA curves (Fig. 5(a)) are given in the Table 4. First two stages lead to production of carbonaceous residue, which is stable at lower temperatures, but is oxidized at higher temperature [24]. In nitrogen atmosphere there are only two stages as can be seen from Fig. 5(b), the first stage (upto 265^{o}C) with 8% mass loss and second stage in the temperature range (359 - 522^{o}C) with 62% mass loss leaving 29.9% char reside at 900 ^{o}C . The first mass loss is similar to that of the one in air atmosphere indicating that this stage is independent of the presence of oxygen. The second stage occurred over a longer temperature range compared to the one in air due to decomposition and release of various fragments over different temperature ranges [22]. On the other hand, in air, some fragments begin to be oxidized whilst the resin is decomposing. The associated EGA results given in Table 5 corroborate these observations. In air, there is no consumption of oxygen during the first stage (below 265^{o}C), oxygen being consumed from 389 – 657^{o}C, which is between the halfway of the

second mass loss stage up to the third char oxidation stage. However, in nitrogen atmosphere (see Fig. 5(b)) there is no char oxidation stage and thus no consumption of oxygen. Similarly the temperature ranges of CO (430 – 650^{o}C) and CO_2 (371 - 657^{o}C) production given in Table 5 coincide with the temperature ranges of decomposition and char oxidation stages of epoxy resin and overlaps the oxygen consumption temperature range. Oxygen consumption in nitrogen atmosphere is absent as expected. The percentage of residual char at 700^{o}C in nitrogen is much higher than that in air atmosphere (see Table 4) due to formation of a stable char. In Fig. 5(b) CO and CO_2 are hardly discernable in nitrogen. Fig. 5(c), which uses an expanded y-axis, shows depletion of CO and CO_2 probably due to generation of other volatile gases from epoxy resin.

3.4 Effect of flame retardants on thermal degradation of epoxy resin and evolved gases

The inclusion of flame retardants in the resin changes its decomposition process, depending upon the type of flame retardant used. Figs. 6-8 give examples of mass loss and CO_2 and CO evolution curves for epoxy resin containing APP (phosphorus containing), RDP (organophosphorous) and FR 245 (phosphorus and halogen-containing), respectively flame retardants with data tabulated for all systems in Tables 4 and 5.

Thermal degradation

The results for all resin-FR combinations, identified in Table 2, are listed in Table 4 in terms of stepwise thermal degradation data. Fig. 6 and Table 4 show that the APP

containing samples start losing mass at slightly higher temperature (199-201^{o}C) than the epoxy resin (193^{o}C). Similar behaviour is observed for other phosphorus and nitrogen containing and organophosphorus flame retarded samples (see Fig. 7(a)), which show a slight delay (5 – 10^{o}C) in the onset of mass loss (first stage in Table 4). This delay indicates the effect of the flame retardant additives on the curing and dehydration of the epoxy resin. On the other hand halogenated flame retardants at 4% level, do not show this effect and even at the 8% level, the effect is minimal.

The onset of decomposition (second stage) temperature for epoxy resin at 354^{o}C is lowered by presence of APP to 316^{o}C at 4% and 303 at 8% levels. Above 400^{o}C, APP increases char formation tendency with increasing level of APP from 4 to 8%, Fig. 6(a). All flame retardants lower the onset temperature of the decomposition stage (see Table 4 and Figs. 6-8). This effect is more pronounced in halogenated flame retardants as seen from Table 4 and Fig. 8(a) where the 4% level shows a reduction in onset temperature by 60 – 80^{o}C. This is reduced by a further 10^{o}C at the 8% level. However, all the flame retardants have a minimal effect on the total mass loss during this stage.

Among the P- and N– containing and organophosphorus flame retardants, the temperature range of the char oxidation stage (457-617^{o}C in epoxy resin, Fig. 6(a)) was prolonged by the presence of a phosphorous group (431-716^{o}C). This is longer the higher the concentration of phosphorous, as seen from Table 4 and Fig. 7(a). This effect is minimal in case of halogenated flame retardants, Fig. 8(a). All phosphorus- containing flame retardants promote char formation, eg., APP increases char yield from 2.5% in pure resin to 7.8% with 4%, and 13.5% with 8% flame retardant. Similarly melamine phosphate increases the amount of char produced by 4.3% and 7.2%, melamine pyrophosphate 4.5%

and 7.1%, RDP 6.6% and 6.9%, BAPP 4.2% and 5.6%. Among the halogenated flame retardants, FR 372 shows an increase in char formation (5.4% and 6.7%), whereas, FR245 has a minimal effect (2.5% and 3.2%). The enhanced char formation in the FR 372 (tris(tribromoneopentyl)phosphate) was due to the presence of phosphorus group along with bromine in the flame retardant.

Carbon dioxide :

Changes in the thermal degradation mechanism can also be observed from Fig. 6(b) and Table 5, where the presence of 4% APP results in a delay in initiation of CO_2 production from 371^oC in the pure resin to 420^oC in the sample E-APP (4). CO_2 production is significantly reduced in the decomposition stage (316 – 451^oC, Table 4) as can be seen from Figs. 6(b) and 9(a). At the 8% APP level, no carbon dioxide is produced during the decomposition stage (303 – 442^oC) (see Fig. 6(b)). The CO_2 production is also reduced during the char oxidation stage. Similar behaviour is observed for all other P- and N-containing retardant samples. Table 5 and Fig. 10 show that the epoxy resin starts producing CO_2 before 400^oC as does the melamine phosphate system. All other flame retardants delay the release of CO_2.

Organophosphorous flame retardants resulted in the highest reduction in CO_2 production during decomposition stage as compared to those of the control resin and the P- and N-containing flame retardants, Figs. 7(b) and 9(a). Simultaneously the initiation temperature of CO_2 production is shifted to higher temperatures, Fig. 10 and Table 5. As a consequence, these flame retardant formulations produce less CO_2 overall as compared to the control resin. Epoxy resins containing the RDP and BAPP retardants produce around

57% CO_2, which is about 20% less than did the control epoxy (see Fig. 11). A higher concentration (8%) of RDP or BAPP did not result in any significant change.

In halogenated combinations, except for the 4% FR 245 sample, no CO_2 was produced during the decomposition stage as seen from Figs. 8(b) and 9(a). During char oxidation stage, the halogenated flame retardants produced more CO_2 than did the control sample. This effect is opposite to that observed for the phosphorus-containing flame retardants. The addition of 4% FR372 or FR245 increased the total CO_2 production from the epoxy resin from 71.2% to 78.8% and 73.4%, respectively. Further addition of FR245 had no significant effect, but the E-FR372(8) system did show a reduction in total CO_2, compared to that obtained from the E-FR372(4) system although the measured level was still higher than that of control, Table 5.

All the various sample combinations, at 8% level resulted in little or no CO_2 production or negligible amounts during second stage degradation (up to 457^{o}C). Samples with organophosphorous flame retardants produced the lowest quantities of total CO_2 with a notable shifting of the initiation temperature for CO_2 production, Figs. 10 and 11. Halogenated flame retardants on the other hand increased CO_2 production were least effective in this respect presumably because they cause little condensed phase reaction. This is discussed more fully in Section 3.5.

Carbon monoxide :

The production of carbon monoxide (CO) is significantly influenced by addition of flame retardants into the resin due to the resultant reduction in combustion efficiency. The total

CO production was 2.9% for the epoxy resin alone, Table 5 and Fig. 6(c). Addition of P-, N- containing flame retardants resulted in an increase in CO production both in decomposition and char oxidation stages, Figs. 9 (a, b). This again is concentration dependent. Addition of higher quantities of flame retardant increased the quantity of CO produced except for the E-MPP(8) system which showed a slight decrease compared to E-MPP(4). The E-MP (8) system evolved the largest amount of CO. In general there was no real trend for these samples. APP at 8% level did not affect the initiation of CO production (see Table 5) compared to epoxy resin (430^{o}C), whereas the melamine phosphate lowered it to 389^{o}C. Melamine pyrophosphate at 4% level lowered the temperature to 414, whereas at 8% level this temperature increased to 494^{o}C.

Organophosphorous flame retardants had a similar effect to that of the P-, N- containing flame retardants, Fig. 7(c) and Table 5. However, there was a significant difference in the initiation temperature of CO production between samples with 4% and 8% concentrations of organophosphorous flame retardants. For the 4% concentration, initiation was at least 30^{o}C earlier than for the control whereas for 8% it was at least 40^{o}C later. However as compared to E-BAPP (4), higher concentration of BAPP had minimal effect in enhancement of total CO production value.

All halogenated flame retardant combinations, except E- FR245 (8), produced less CO compared to the P-, N- containing and organophosphorus flame retardant combinations, Fig. 12.

Oxygen consumption :

Oxidation of the resin structure generally starts during the second decomposition stage, Tables 4 and 5. The epoxy resin consumes nearly 140% of oxygen for every 100% of resin. The oxygen consumption decreases with the addition of flame retardants. Zaharescu [25] also observed that the inclusion of flame retardants reduces the average oxygen consumption. The effect was greater the higher the proportion of flame retardants added. As seen from Table 5, organophosphorus flame retardants at 8% concentration resulted in the largest reduction in oxygen consumption compared to the control resin.

3.5 Discussion

(i) Effect of phosphorous and nitrogen containing flame retardants :

All the phosphorous and nitrogen based flame retardants delayed the onset temperature of the initial mass loss (except for MP at 8% level). This could be due to the effect of these flame retardants on curing and hindrance of dehydration by melting flame retardant chemicals and hence, a lower mass loss was observed for this stage. APP starts melting around 200^{o}C [26] followed by dehydration and crosslinking into polyphosphate around 240^{o}C [27], whereas melamine phosphate and pyrophosphate undergo pseudo-melting, and dehydration above 220 and 280^{o}C, respectively [27, 28]. The onset temperature in main decomposition was reduced due to the degradation of flame retardants which leads to formation of denser char. APP starts degrading around 260^{o}C producing phosphoric acid, which polymerises at higher temperatures to polyphosphoric acid [27]. Melamine phosphate and melamine pyrophosphate undergo dehydration starting from 220 and 280^{o}C, respectively and decomposition starting from 350 and 380^{o}C, respectively to form

different phosphates [29]. Thus phosphorus- based flame retardants in general, react in the condensed phase producing phosphoric acid and/or polyphosphosphoric acid [32] which enhance char forming reactions [22, 27-29]. These reactions interrupt the diffusion of oxygen into the system resulting in incomplete combustion [31]. This effect is enhanced by increasing flame retardant concentration. As a result, CO_2 production is reduced and that of CO enhanced. Char formation enhanced by phosphorous-containing flame retardants, acts as a barrier on the surface of the polymer restricting interaction with oxygen and further oxidation [30]. This restricts the conversion from CO to CO_2 [31] resulting in more CO production. Thus the O_2 consumption is reduced. The higher CO_2 production observed during the decomposition stage of melamine phosphate system (Fig. 9) could be due to the fact that it decomposes in the temperature range from 350 to 500^oC to produce ammonia and phosphate and hence is not effective in the temperature range 307-384 ^oC.

(ii) Effect of organophosphorous flame retardants :

The organophosphorous flame retardants act in a similar way to the aliphatic phosphorous-containing flame retardants in delaying the degradation during the curing stage. However, mass loss in the first stage is slightly higher than that of P- and N- based flame retardant, which may be due to the liquid form of these flame retardants, which does not interfere with the dehydration reactions of resin. Although the systems containing organophosphorous flame retardants decomposed in a more or less similar manner to the P- and N- based flame retardant systems, the production of CO_2 is much less both during the decomposition stage and the overall degradation, see Figs. 9(a) and 11 respectively. RDP and BAPP start decomposing from 270 and 365^oC, respectively

releasing condensed phase active phosphoric acid groups. Aromatic phosphorous groups are much more reactive [34] than aliphatic phosphorous groups and would, therefore, be expected to show a greater extent of interaction with oxygen. As a consequence, lower amounts of CO and CO_2 were detected from these organophosphorus systems. The greater effectiveness of organophosphorous flame retardants in reducing CO and CO_2 production could be due to the better dispersion of these liquid flame retardants in the resin structure. The bulky phosphorus-resorcinol or phenol-groups of the flame retardants hinder the diffusion of oxygen into the resin system thus reducing oxidatation to CO_2 [35]. As Table 5 indicates the organophosphorus flame retardant systems had a significant reduction in oxygen consumption which is one third of that of control resin.

(iii) Effect of halogenated flame retardants :

The halogenated flame retardants work differently than phosphorous containing flame retardants. They act in vapour phase, producing free radicals which interact with decomposing polymers and reduce the degradation. The early degradation observed for the halogenated flame retardant system could be due to dehydration and chain scission by the halogen group. The flame retardants FR 372 and FR 245 used in this work melt at 180 and 229^{o}C, and decompose at 270 and 310^{o}C, respectively as observed from their differential thermal and thermogravimetric results. The much earlier decomposition of the resin in the presence of a halogenated flame retardant could be due to a radical chain mechanism initiated by the Br group initiating reaction leading to HBr formation [36]. Halogens are known to inhibit oxidation/combustion in the vapour phase. This does not affect the char formation or CO_2 evolved from the system. In the current experiments, these flame retardants increased the CO_2 and CO production with respect to the control

resin. The E-FR245 (8) produced comparatively more CO than did any of the other halogenated combinations. This could be due be to the presence of a C-N bond in FR-245 the consequence of which is an incomplete reaction to form CO [37]. FR 372 is tris(tribromoneopentyl)phosphate, the presence of phosphorous in the flame retardant helps in condensed phase producing more char formation, as can be seen from Table 5. FR 245 on the other hand has no effect on char residue.

4. Conclusions

A quantitative and qualitative technique has been developed which can measure CO and CO_2 at different stages of thermal degradation of a polymer and temperature ranges of their production. The results have been verified by testing inorganic materials with known thermal history. For epoxy resin system, the calculated values sum up to 100% of mass, thus providing confidence in results. The results obtained from the TGA-EGA experiments show that inclusion of phosphorus based flame retardants slows down the resin degradation and enhances the char formation at higher temperatures. It affects the gaseous species involved with resin during thermal degradation in three ways: (i) it reduces the total CO_2 production as well as delaying the initiation of CO_2 production during decomposition, (ii) CO production is increased due to incomplete combustion resulting from the presence of the flame retardant, (iii) oxygen consumption is reduced due to reduced interaction of reactive bonds and lower conversion of CO to CO_2. Organophosphorous flame retardants work in a similar manner as to P- and N- containing flame retardants, but produce less CO_2 and CO. The vapour phase activity of halogenated flame retardants is supported by the limited effect of these systems on CO and CO_2 production.

References :

1. Fire Statistics, United Kingdom, 2004, Office of the Deputy Prime Minister, London, OPDM Publications, ISBN 13 – 978 185 112 8433, February, 2006. p. 13.
2. Hull TR, Quinn RE, Areri IG, Purser DA. Combustion toxicity of fire retarded EVA. Polym Degrad and Stab 2002; 77 (2): 235-242.
3. Hull R, Wills CL, Artingstall T, Price D, Milnes GJ. In: Le Bras M, Wilkies C, Bourbigot S, editors. Fire Retardancy of Polymers. New Applications of Mineral Fillers. Cambridge: RSC, 2005. Chapter 28.
4. BS 2782-1: Method 140A: 1992, ISO 1210:1992, Plastics — Part 1: Thermal properties — Method 140A: Determination of the burning behaviour of horizontal and vertical specimens in contact with a small-flame ignition source.
5. BS EN ISO 4589 – 2 : 1999, Plastics – Determination of burning behaviour by oxygen index – Part 2: Ambient temperature test.
6. BS 476-15:1993, ISO 5660-1:1993, Fire tests on building materials and structures. Method for measuring the rate of heat release of products.
7. Slager TL, Prozonic FM. Simple methods for calibrating IR in TGA/IR analyses. Thermochim Acta 2005; 426 (1-2): 93-99.
8. Xie W, Pan WP. Thermal characterization of materials using evolved gas analysis. J Therm Anal Cal 2001; 65: 669-685.
9. Kaisersberger E, Post E. Practical aspects for the coupling of gas analytical methods with thermal-analysis instruments. Thermochim Acta 1997; 295: 73-93.

10. Wendlandt WW. In: Elving PJ, Winefordner JD, Kolthoff IM, editors. Chemical Analysis, Thermal Analysis, 3rd edition. New York: John Wiley and Sons, 1985. p. 469-588
11. Davidson RG. Enhancement of evolution profiles in pyrolysis-evolved gas-infrared spectroscopy of polymers. J Anal Appl Pyrol 1989; 16: 143-152.
12. Mittleman M. Quantitative TG/IR. Thermochim Acta 1990; 166: 301-308.
13. Price D, Horrocks AR, Akalin M. Use of DTA with infrared analysis of evolved gas to investigate the effect of flame retardants on gas evolution from pyrolysed cellulose (cotton). Brit Polym J 1988; 20: 61-67
14. Horrocks AR, Price D, Akalin M. FTIR analysis of gases evolved from cotton and flame retarded cotton fabrics pyrolysed in air. Polym Degrad and Stab 1996; 52: 205-213.
15. Lee H, Neville K. Handbook of Epoxy Resin. New York: McGraw-Hill Book Company, 1967. Chapter 1, p. 5 - 22
16. May CA, Tanaka Y. Epoxy Resins, Chemistry and Technology. New York: Marcel Dekker, 1973. Chapter 8, p. 719–782.
17. McAdams LV, Gannon JA. In: Mark HF, Bikales NM, Overberger CG, Menges G, editors. Encyclopedia of Polymer Science and Engineering, 2nd edition, Vol. 6: Epoxy resins. USA: Wiley Interscience publication, 1988. p.322-382.
18. Weil ED, Levchik SV. A review of current flame retardant systems for epoxy resins. J Fire Sci 2004; 22: 25-40
19. Biswas B, Kandola B and Horrocks AR, to be presented at 11th European Meeting on Fire Retardant Polymers, FRPM'07, Bolton, UK, 4-6 July, 2007.

20. Sills ID, He S. Determination of evolved gas transfer time from a thermoanalyser to a coupled gas detection system using pyrite oxidation. Thermochim Acta 1999; 339 (1-2): 125-130
21. Zhang S, Horrocks AR, Hull R, Kandola BK. Flammability, degradation and structural characterization of fibre-forming polypropylene containing nanoclay–flame retardant combinations. Polym Degrad and Stab 2006; 91 (4): 719-725
22. Kandola BK, Horrocks AR, Myler P, Blair D. Thermal Characterization of Thermoset Matrix Resin. In : Nelson GL, Wilkie CA, editors. Fire and Polymers, ACS Symp Ser 797; Washington : 2001. p 344-360.
23. Evans SJ, Haines PJ, Skinner GA. The effects of structure on the thermal degradation of polyester resins. Thermochimica Acta 1996; 278 (1-2): 77-89
24. Liu YL, Hsiue GH, Lan CW, Chiu YS. Phosphorus-containing epoxy for flame retardance: IV. Kinetics and mechanism of thermal degradation. Polym Degrad and Stab 1997; 56 (3): 291-299
25. Zaharescu T. New assessment in thermal degradation of polymers. Polymer Testing 2001; 20 (1): 3-6
26. Camino G, Costa L, Luda MP. Mechanistic aspects of intumescent fire retardant systems. Macromol Chem, Macromol Symp 1993; 74: 71-83
27. Kandola BK, Horrocks AR. Complex char formation in flame-retarded fibre-intumescent combinations—II. Thermal analytical studies. Polym Degrad Stab 1996; 54 (2-3): 289-303
28. Horrocks AR, Davies PJ**.** Char formation in flame-retarded wool fibres. Part 1. Effect of intumescent on thermogravimetric behaviour. Fire Mater 2000; 24 (3): 151-157.
29. Kandola BK, Horrocks AR, Horrocks S**.** Char Formation in Flame-Retarded Fibre-

Intumescent Combinations. Part V. Exploring Different Fibre/Intumescent Combinations. Fire Mater 2001; 25 (4): 153-160

30. Hörold S. Phosphorus flame retardants in thermoset resins. Polym Degrad and Stab 1999; 64 (3): 427-431
31. Lewin M, Weil E. In: Horrocks AR, Price D, editors. Fire Retardant Materials, Mechanisms and modes of action in flame retardancy of polymers. Cambridge: Woodhead Publication 2003. Chapter 2, p.31-68.
32. Chiu SH, Wang WK. Dynamic flame retardancy of polypropylene filled with ammonium polyphosphate, pentaerythritol and melamine additives. Polymer 1998; 39 (10): 1951-1955.
33. Hull TR, Wills CL, Lebek K, Paul K, Price D. Methodology for Small-Scale Toxic Hazard Assessment of Burning Cables. In: Wilkie CA, Nelson GL, editors. Fire and Polymers IV Materials and Concepts for Hazard Prevention, ACS Symp Ser 922; Washington : 2006. p 348-363.
34. Wang CS, Lin CH. Synthesis and properties of phosphorus containing advanced epoxy resins. J Appl Polym Sci 2000; 75 (3): 429-436
35. Levchik SV, Piotrowski A, Weil E, Yao Q. New developments in flame retardancy of epoxy resins. Polym Degrad and Stab 2005; 88 (1): 57-62
36. Balabanovich AI, Hornung A, Merz D, Seifert H. The effect of a curing agent on the thermal degradation of fire retardant brominated epoxy resins. Polym Degrad Stab 2004; 85 (1): 713-723
37. Sullivan JM, Axworthy AE, Houser TJ. Kinetics of the gas-phase pyrolysis of poly(difluoramino) fluoromethanes. J Phys Chem, 1970; 74 (13): 2611-2620

Captions for Tables

Table 1. Mass percentages of various components in the formulations

Table 2. Sample description

Table 3. TGA-EGA results for sodium bicarbonate ($NaHCO_3$) and calcium carbonate ($CaCO_3$)

Table 4. Mass loss percentage of samples in different stages from TGA curves in air

Table 5. TGA-EGA results in air atmosphere

Captions for Figures

Fig. 1. Time delay measurement in EGA by injecting CO_2 into the TGA at 20 ml/min.

Fig. 2. TGA-EGA curves of (a) 5.13 mg $NaHCO_3$ and (b) 5.582 mg $CaCO_3$ in air atmosphere at 20 ml/min flow rate

Fig. 3. Experimental and calculated oxygen concentrations in evolved gases from sodium bicarbonate ($NaHCO_3$) during TGA-EGA in air atmosphere

Fig. 4. Typical curve of gas generated from TGA-EGA results.

Fig. 5. TGA-EGA of epoxy resin in flowing (a) air and (b) nitrogen atmosphere at 20 ml/min and (c) CO and CO_2 evolution of epoxy resin in air and nitrogen

Fig 6 (a) Mass Loss (b) CO_2 and (c) CO production of epoxy resin and the resin with 4% and 8% APP

Fig. 7. (a) Mass Loss (b) CO_2 and (c) CO production of epoxy resin and the resin with 4% and 8% RDP

Fig. 8. (a) Mass Loss (b) CO_2 and (c) CO production of epoxy resin and the resin with 4% and 8% FR245

Fig. 9. Carbon dioxide (CO_2) and carbon monoxide (CO) evolution during a) decomposition stage (temp. range 265 – 460 ^oC) and b) char oxidation stage (temp. range 420 – 720 ^oC) of epoxy resin without / with flame retardants.

Fig. 10. Temperature ranges of carbon dioxide (CO_2) and carbon monoxide (CO) evolution of epoxy resin without / with flame retardants

Fig. 11. Difference in total CO_2 production between epoxy resins containing 4% and 8% flame retardants from the unmodified resin.

Fig. 12. Difference in total CO production between epoxy resins containing 4% and 8% flame retardants from the unmodified resin.

Table 1 Mass percentage of various components in the formulations

Samples	Epoxy resin	DDS	PES	FR
Epoxy resin	57.8	22.2	20	-
96% Epoxy + 4% FR	57.8	22.2	16	4
92% Epoxy + 8% FR	57.8	22.2	12	8

Table 2 Sample description

Sample code	Flame retardants		Epoxy formulation* (%)
	Name	(%)	
E-100	-	-	100
E-APP (4)	APP	4	96
E-APP (8)	APP	8	92
E-MP (4)	MP	4	96
E-MP (8)	MP	8	92
E-MPP (4)	MPP	4	96
E-MPP (8)	MPP	8	92
E-RDP (4)	RDP	4	96
E-RDP (8)	RDP	8	92
E-BAPP (4)	BAPP	4	96
E-BAPP (8)	BAPP	8	92
E-FR372 (4)	FR372	4	96
E-FR372 (8)	FR372	8	92
E-FR245 (4)	FR245	4	96
E-FR245 (8)	FR245	8	92

Note : '*' Epoxy resin + DDS + PES (see Table 1)

Table 3 TGA-EGA results for sodium bicarbonate ($NaHCO_3$) and calcium carbonate ($CaCO_3$)

Sample	Medium	Sample mass (mg)	Expected CO_2 generation (mg)	Experimental			CO_2 generation (%)
				CO_2 generation (mg)	CO generation (mg)	O_2 consuption (mg)	
$NaHCO_3$	Air	5.13	1.34	1.34	-	-	26
	Nitrogen	5.04	1.31	1.31	-	-	26
$CaCO_3$	Air	5.58	2.45	2.42	-	-	44
	Nitrogen	9.75	4.29	4.29	-	-	44

Table 4 Mass loss percentages of samples in different stages from TGA curves in air

Sample	1st Stage		2nd Stage		3rd Stage		Char at 700°C (%)
	Temp Range (°C)	Mass Loss (%)	Temp Range (°C)	Mass Loss (%)	Temp Range (°C)	Mass Loss (%)	
ER (100)	193-265	10	354-457	30	457-617	57	2.5 (29.9)
Epoxy with P- and N- based FRs							
E-APP (4)	201-259	6	316-451	29	451-652	57	7.8 (34.8)
E-APP (8)	199-254	5	303-442	28	442-716	53	13.5
E-MP (4)	199-246	6	307-452	30	452-638	59	4.3 (32.5)
E-MP (8)	186-241	6	291-448	31	448-702	56	7.2
E-MPP (4)	204-259	6	307-445	30	445-637	58	4.5 (34.2)
E-MPP (8)	214-258	3	307-439	34	439-678	55	7.1
Epoxy with organophosphorous FRs							
E-RDP (4)	198-264	8	310-453	31	453-642	54	6.6
E-RDP (8)	193-262	10	294-431	25	431-639	58	6.9
E-BAPP (4)	211-264	6	321-456	32	456-651	55	5.6
E-BAPP (8)	206-265	10	318-446	29	446-657	56	4.2
Epoxy with halogenated FRs							
E-FR372 (4)	184-263	8	277-434	29	434-619	57	5.4
E-FR372 (8)	197-263	6	268-432	30	432-635	57	6.7
E-FR245 (4)	190-266	8	297-456	35	456-628	54	2.5
E-FR245 (8)	201-261	5	285-428	31	428-628	61	3.2

Note : Values in the parentheses are char residues in nitrogen atmosphere.

Table 5 TGA-EGA results in air atmosphere

Sample	O_2 Consumption		Evolved Gases				Char %
	Temp Range	Parts*	CO_2		CO		
			Temp	%	Temp	%	
ER -100	389-657	140.3	371-657	71.2	430-650	2.9	1.04
Epoxy with P- and N- based FRs							
E-APP (4)	396-714	129.8	420-714	60.5	453-632	4.4	3.39
E-APP (8)	484-756	103.6	484-758	67.6	432-657	6.8	6.63
E-MP (4)	380-665	127.3	384-652	69.2	398-642	3.1	1.89
E-MP (8)	372-691	122.5	479-718	67.1	389-716	10.1	3.24
E-MPP (4)	391-686	125.9	400-701	65.6	414-667	6.4	1.99
E-MPP (8)	359-682	126.8	411-679	66.0	494-682	5.7	3.13
Epoxy with organophosphorous FRs							
E-RDP (4)	352-653	132.1	433-651	57.1	391-642	4.5	2.84
E-RDP (8)	406-662	93.9	498-659	58.3	493-633	4.9	3.56
E-BAPP (4)	401-651	122.4	439-651	56.1	402-651	5.1	2.52
E-BAPP (8)	409-660	92.0	494-653	57.8	471-669	5.5	2.19
Epoxy with halogenated FRs							
E-FR372 (4)	412-614	97.2	474-634	78.8	468-619	4.9	2.74
E-FR372 (8)	201-639	127.1	479-647	71.9	451-568	3.2	2.95
E-FR245 (4)	349-639	139.0	405-633	73.4	401-638	2.6	1.05
E-FR245 (8)	322-606	118.8	480-616	74.4	414-576	6.1	1.46

* parts per 100 parts of resin

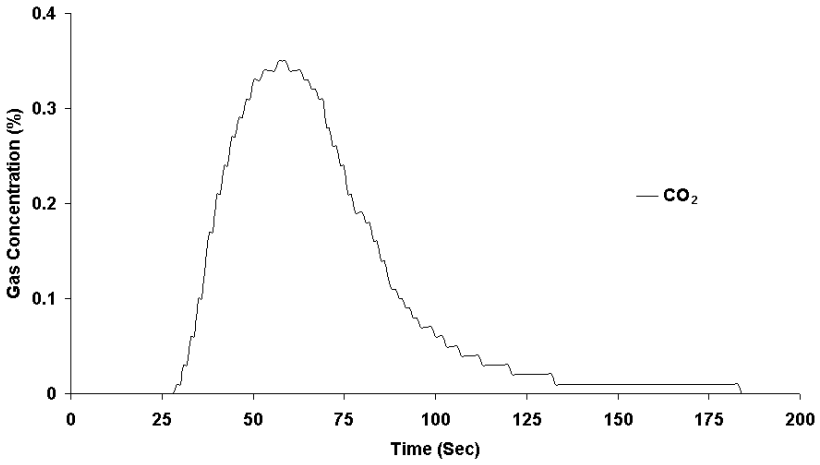

Fig. 1. Time delay measurement in EGA by injecting CO_2 into the TGA at 20 ml/min.

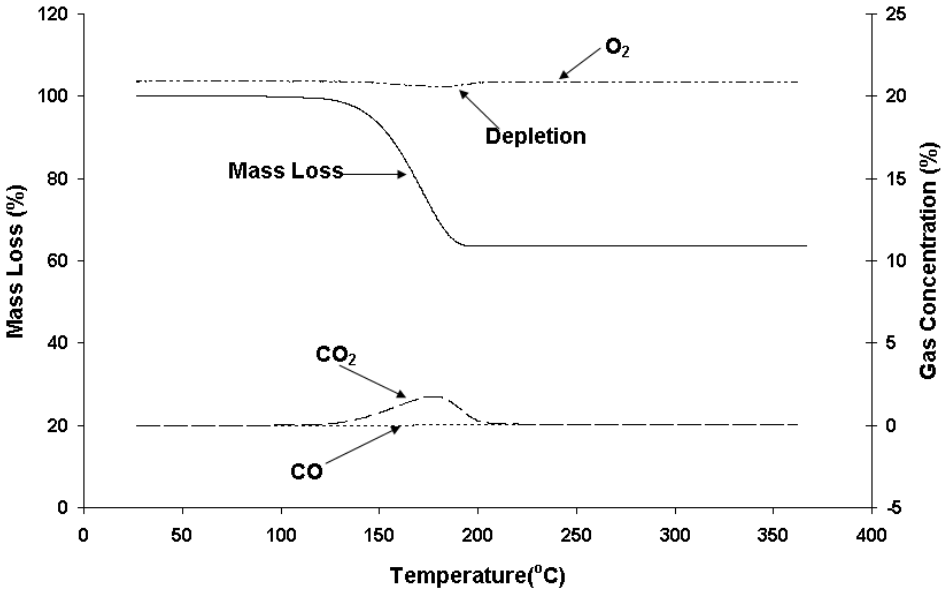

(a)

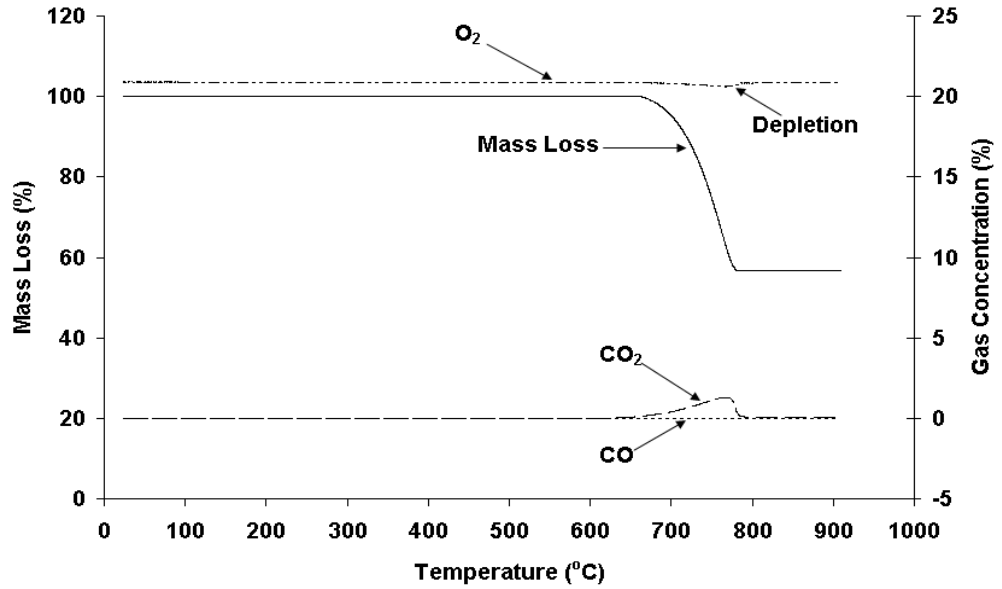

(b)

Fig. 2. TGA-EGA curves of (a) 5.13 mg $NaHCO_3$ and (b) 5.582 mg $CaCO_3$ in air atmosphere at 20 ml/min flow rate

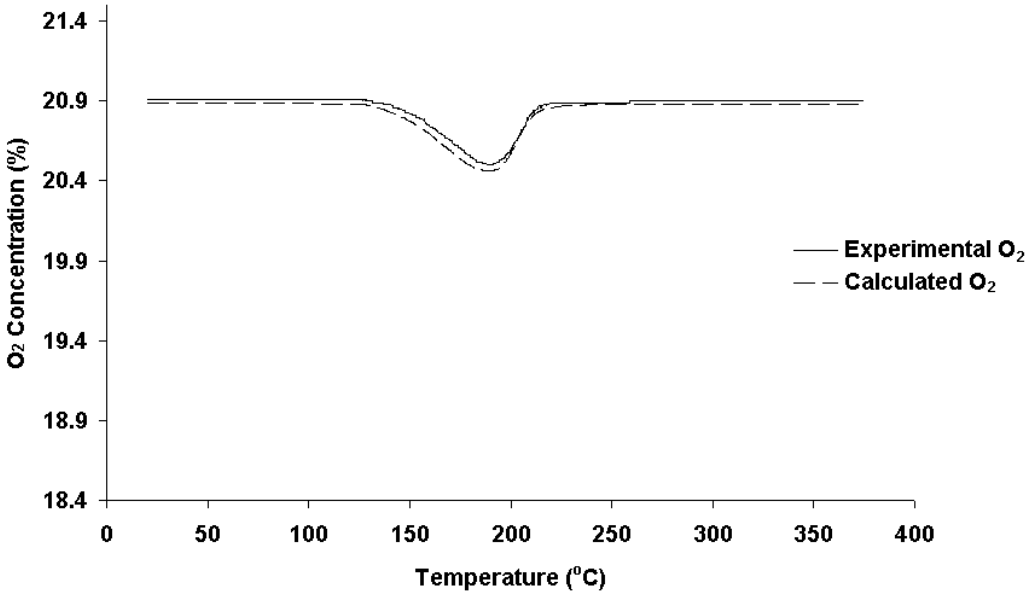

Fig. 3. Experimental and calculated oxygen concentrations in evolved gases from sodium bicarbonate ($NaHCO_3$) during TGA-EGA in air atmosphere

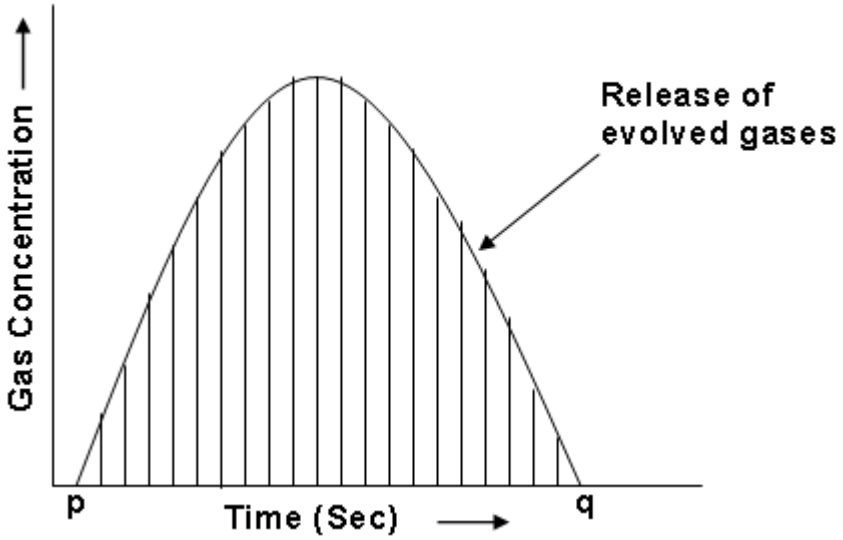

Fig. 4. Typical curve of gas generated from TGA-EGA results.

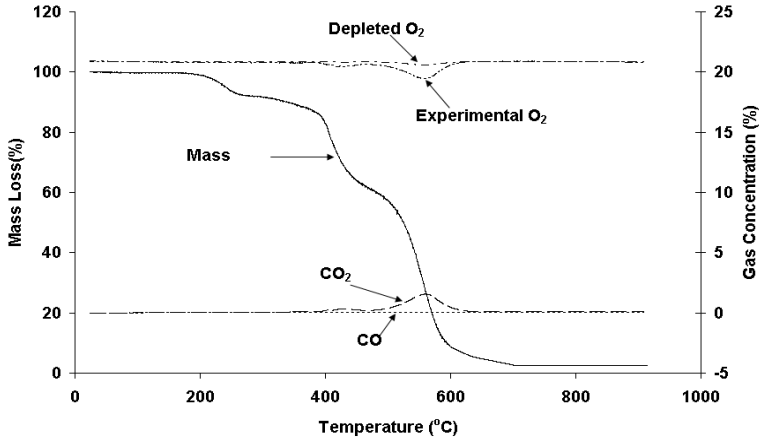

(a)

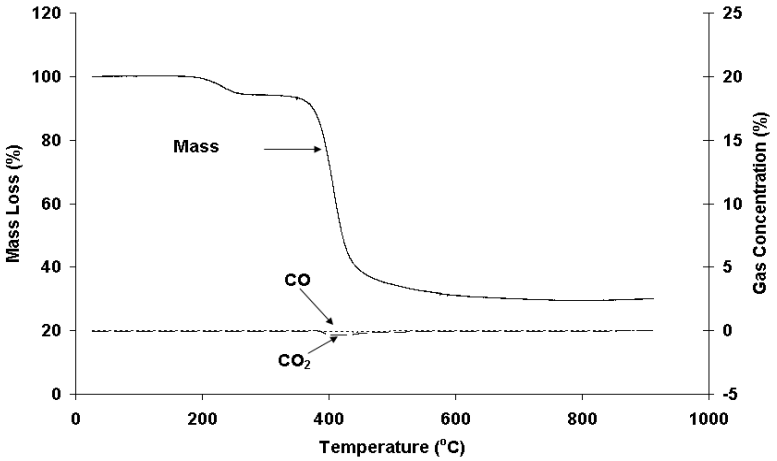

(b)

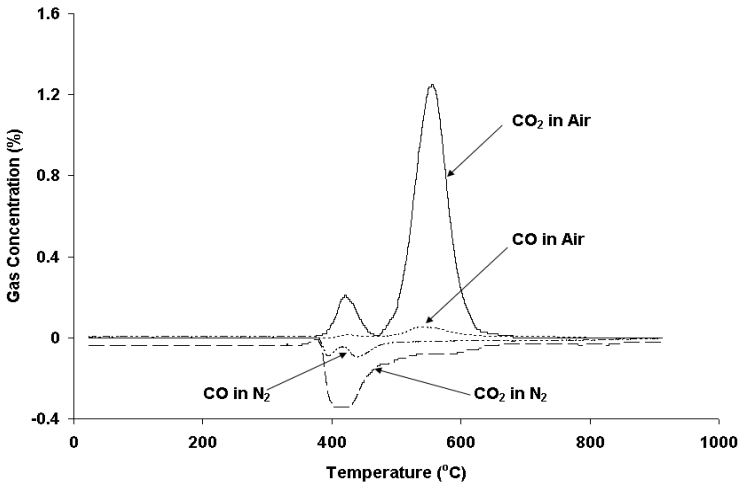

(c)

Fig. 5. TGA-EGA of epoxy resin in flowing (a) air and (b) nitrogen atmosphere at 20 ml/min and (c) CO and CO_2 evolution of epoxy resin in air and nitrogen

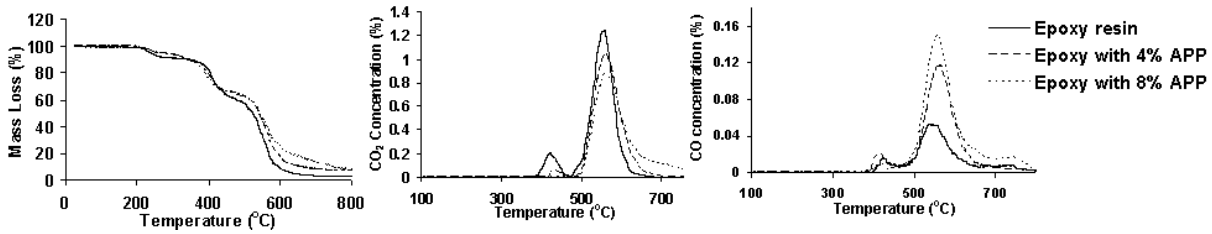

(a) (b) (c)

Fig. 6. (a) Mass Loss (b) CO_2 and (c) CO production of epoxy resin and the resin with 4% and 8% APP

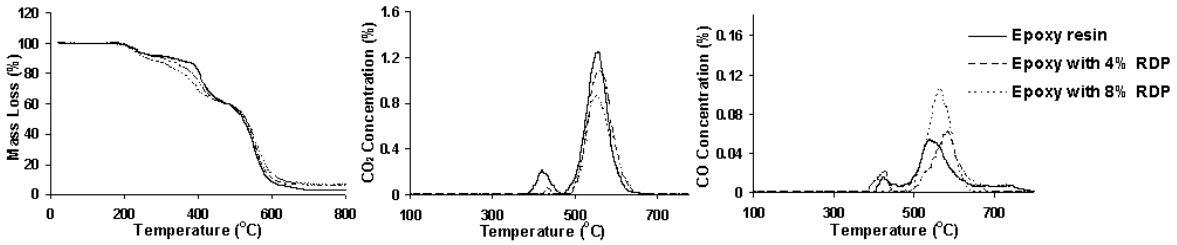

(a) (b) (c)

Fig. 7. (a) Mass Loss (b) CO_2 and (c) CO production of epoxy resin and the resin with 4% and 8% RDP

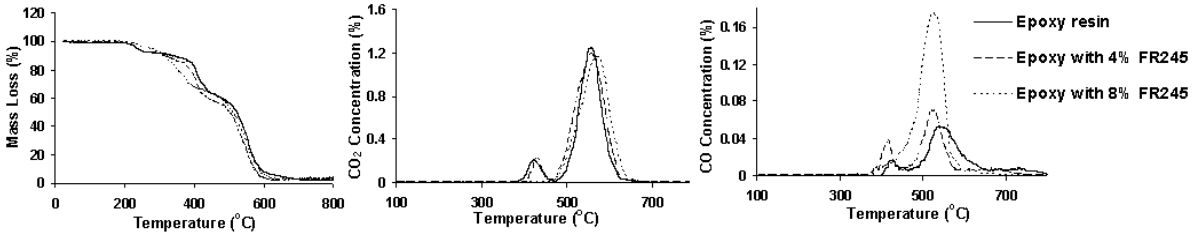

(a) (b) (c)

Fig. 8. (a) Mass Loss (b) CO_2 and (c) CO production of epoxy resin and the resin with 4% and 8% FR245

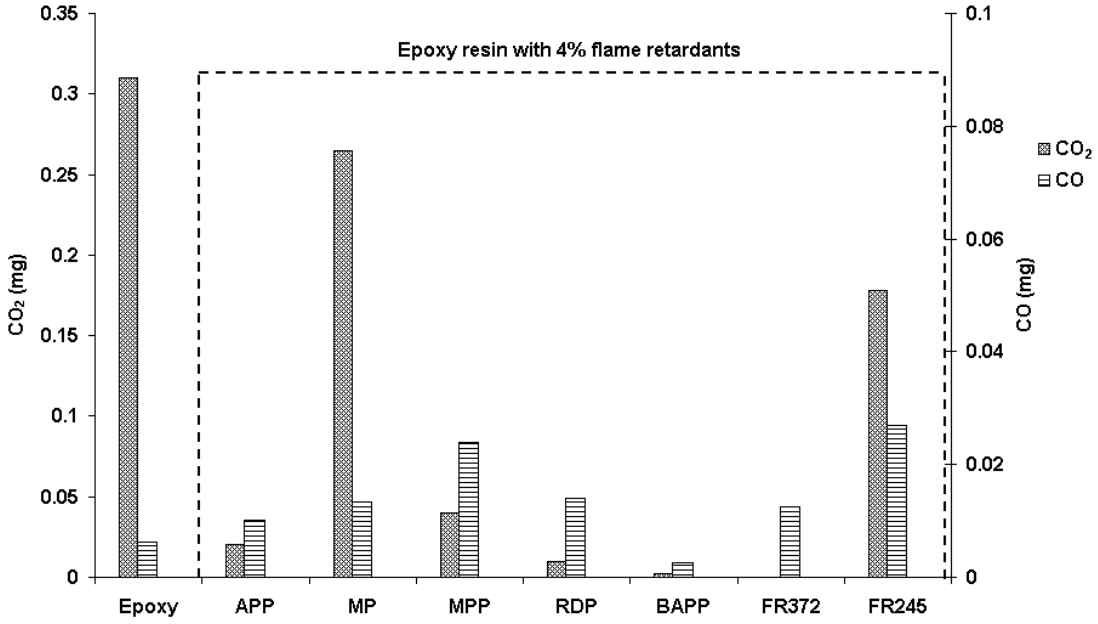

(a)

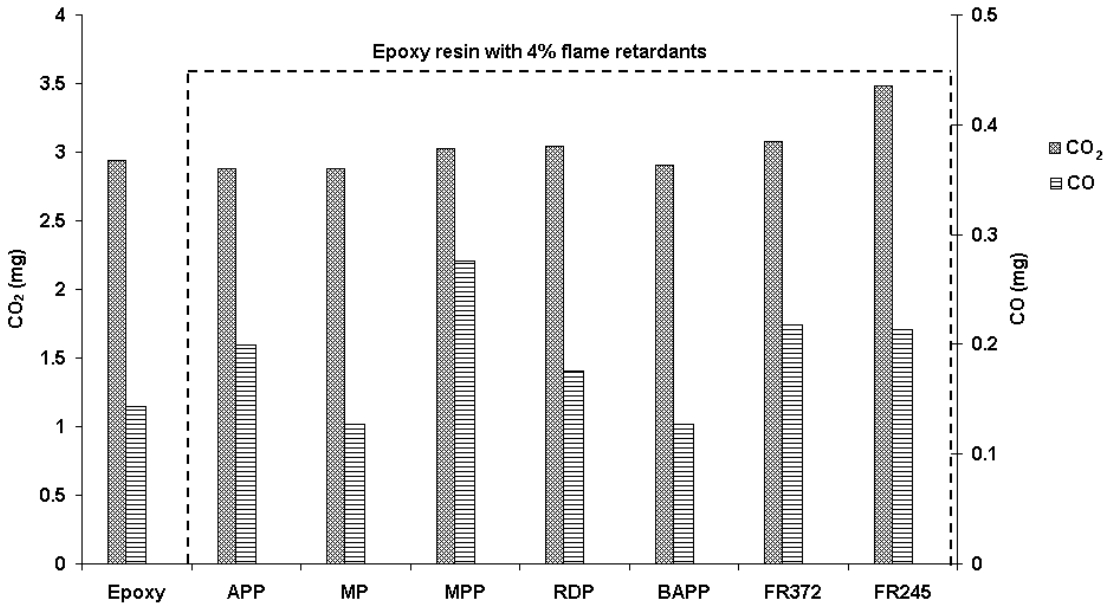

(b)

Fig. 9. Carbon dioxide (CO_2) and carbon monoxide (CO) evolution during a) decomposition stage (temp. range 265 – 460 ^oC) and b) char oxidation stage (temp. range 420 – 720 ^oC) of epoxy resin without / with flame retardants.

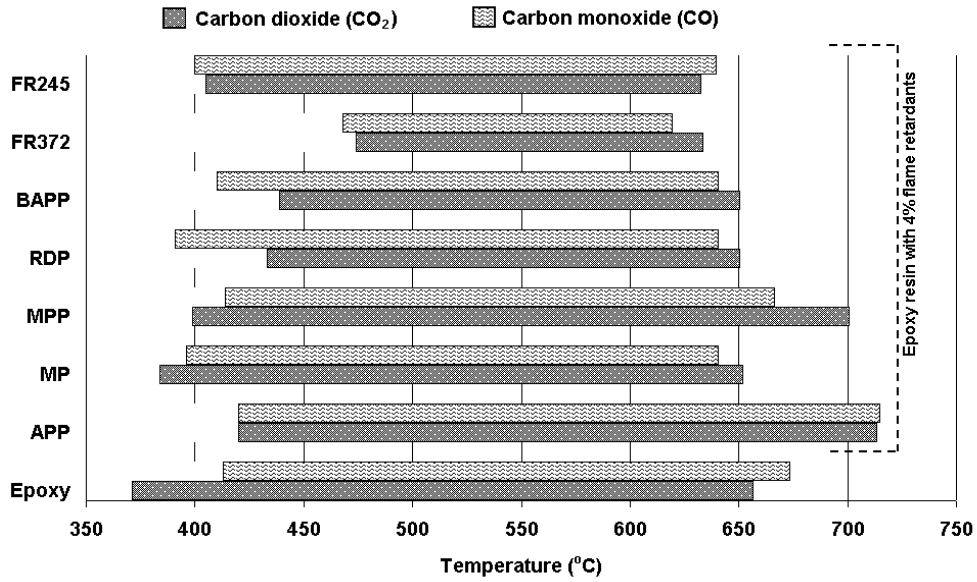

Fig. 10. Temperature ranges of carbon dioxide (CO_2) and carbon monoxide (CO) evolution of epoxy resin without / with flame retardants

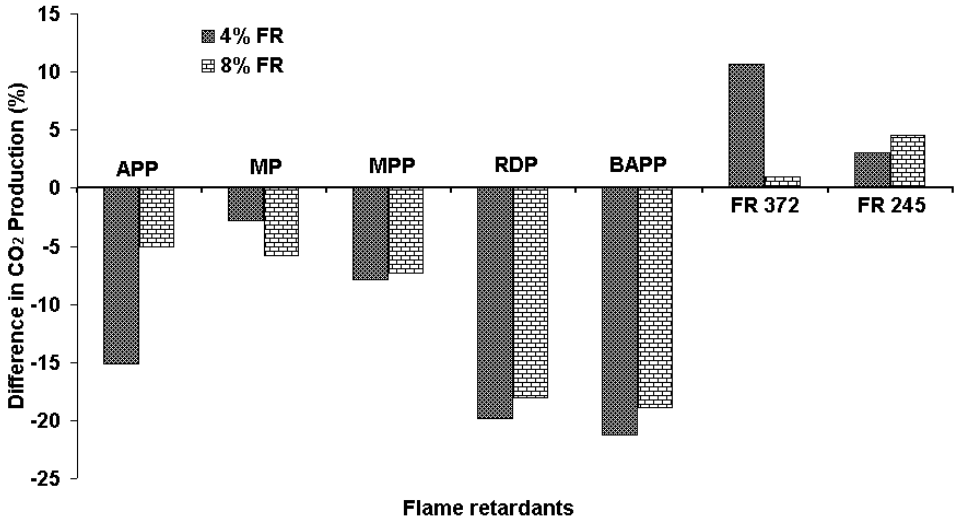

Fig. 11. Difference in total CO_2 production between epoxy resins containing 4% and 8% flame retardants from the unmodified resin.

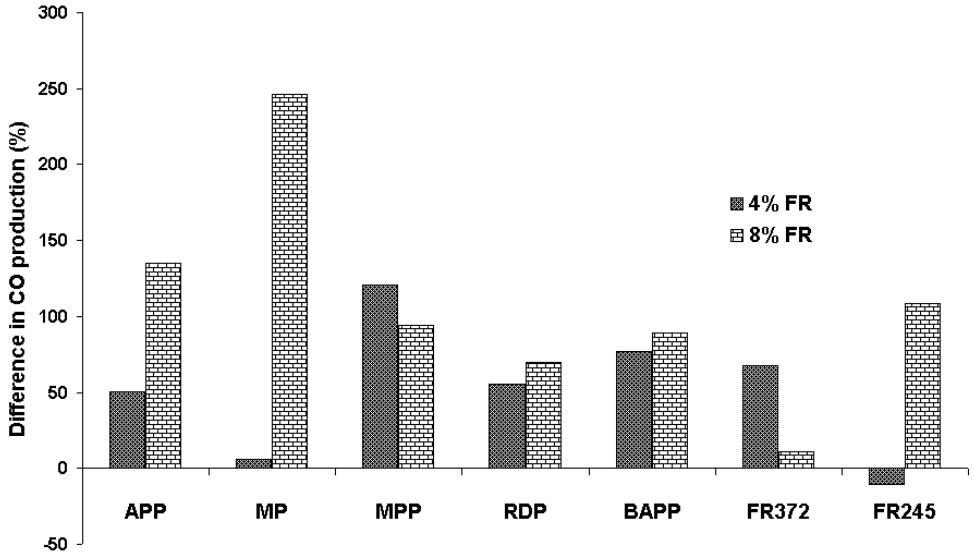

Fig. 12. Difference in total CO production between epoxy resins containing 4% and 8% flame retardants from the unmodified resin.